Conceptual Design and advanced hydro-aero-elastic modeling of a TLP concept for floating Wind Turbine applications

T.P. Mazarakos(*), D. Manolas(**), T. Grapsas(*), S.A. Mavrakos(*), V.A. Riziotis(**) & S.G. Voutsinas(**)

(*)Laboratory for Floating Structures and Mooring Systems, School of Naval Architecture and Marine Engineering, National Technical University of Athens, Greece

(**)Aerodynamic Laboratory, School of Mechanical Engineering, Technical University of Athens, Greece

ABSTRACT: A multi – cylinder TLP design concept of a floating structure is presented for supporting a 5 MW W/T. The present design represents a first step towards the development, at a second stage, of a multi – purpose floating structure for offshore wind and wave energy sources exploitation. Targeting the conceptual design of the proposed TLP floating structure for the 5MW wind turbine, the combined effects of water waves and wind on the floating offshore wind turbine are investigated. At the present stage, a design-oriented solution method for the coupled dynamics of the floating structure in the frequency domain is presented and the corresponding RAO's are calculated. The hydrodynamic characteristics are determined using matched axisymmetric eigenfunction expansions, while the loading (gravitational, inertial and aerodynamic loads) contributed by the WT is projected on the six degrees of the floater motions based on a reduced order model leading to extra mass, damping and stiffness matrices in the dynamic equation of the floater. In addition, time domain fully coupled hydro-servo-aero-elastic simulations are carried out considering wave excitation described by a white noise spectrum whereby the effective RAO's are computed from the corresponding time signals. Comparison between the 2 methods is carried out at the RAO's level and conclusions are drawn.

1 INTRODUCTION

1.1 *The context*

Offshore wind energy is currently attracting most of the research attention within the sector. Most installations presently concern shallow water sites but due to the substantial wind potential in the open sea, it is expected that deep offshore will be next important milestone for the wind energy industry. In this respect the main challenge concerns the design of the supporting structure, meaning the floater and the moorings. Already in the series of the OC IEA Annexes (Jonkman et al., 2010b) the spar buoy concept first designed for the HyWind project and the semi-submersible floater designed and analyzed by Maine University (Goupee et al, 2012) have been investigated. In both cases conventional mooring lines were considered, having in mind deep sea installations. In intermediate depths an alternative would be to have a TLP already proposed in Sclavounos et al. (2006) and Stewart et al. (2012). In the present paper, a multi – cylinder TLP design concept for the support structure of the NREL 5MW RWT is analyzed.

1.2 *The tools*

In the process of designing floating wind energy systems, there is need to develop in parallel on one hand fast running tools that can provide an overview of the design space and on the other hand detailed analysis of the full system with all the underlying mechanisms.

Detailed modeling of floating wind turbines is carried out by hydro-servo-aero-elastic time domain solvers combining appropriate sub-modules in fully coupled mode. Current state-of-the-art models use the blade element momentum (BEM) for the aerodynamic loading, linear hydrodynamic theory for estimating the wave loads, beam structural modeling of the wind turbine components, multi-body dynamics for the complete system and PI based controllers.

An advanced full model along the above lines has been developed at NTUA, known by the name hydroGAST (Riziotis et al., 1997, 2004, Manolas et al. 2012). The specific model has been verified within the OC4 IEA project (Popko et al., 2012, Robertson et al., 2014) while in Manolas et al. (2012, 2014) non-linear effects in the aerodynamic and structural modeling have been thoroughly assessed.

Running fully coupled simulations is expensive in computational terms and therefore in the early design stages a less demanding process is needed. Reduced

order models (ROMs) can be defined in several ways. For dynamic systems the usual choice is to rely on frequency domain models. Targeting the design assessment of the supporting structure, the presence of the wind turbine can be introduced in the motion equations of the floater by appropriately projecting the wind turbine loads to the corresponding degrees of freedom. By linearizing the resulting equations, frequency domain analysis becomes straightforward.

Clearly ROMs constitute a compromise and therefore their validity should be checked. In the present paper, the ROM described in Section 3 is compared to the results produced with the hydroGAST advanced full model.

The program HAMVAB (Mavrakos, 1996), provides the first- order exciting wave forces and motions induced on multiple interaction vertical axisymetric bodies. Hydrodynamic interactions effects are taken into account for solving the diffraction/ radiation problems. The bodies in the arrangement are allowed to move either independently or as a unity. Restoring forces due to elastic springs attached to the cylinders can be incorporated in the solution procedure. Drift forces both on the entire multi-cylinder configuration and on each individual cylinder are calculated using the momentum conservation principle into finite control volumes surrounding each body of the configuration.

2 FLOATING SYSTEM PROPERTIES

The floating system has been defined for the NREL 5MW Reference Wind Turbine. It is a variable- speed variable-pitch controlled WT and the detailed data are given in Jonkman et al. (2009, 2010a). The tower of the wind turbine is cantilevered at an elevation of 10m above the SWL to the top of the main column of the floating platform. The draft of the platform is 20m. The floating platform consists of a main column attached to the tower, and three offset columns that are connected to the main column through a series of smaller diameter pontoons and cross members. There are five sets of these smaller members (members in gray in Figure 1). Two sets of three pontoons (for a total of six members) connecting the offset columns with each other (forming a triangle, both at the top and bottom of the semi). Two sets of three pontoons (for a total of six members) connecting the offset columns with the main column (forming a y-connection, both at the top and bottom of the semi). Three cross braces connecting the bottom of the main column with the top of the offset columns. Each column starts above the SWL and continues beneath the water. A summary of the geometry, including the diameters of each of the members is given in Table 1. These properties are all relative to the un-displaced position of the platform.

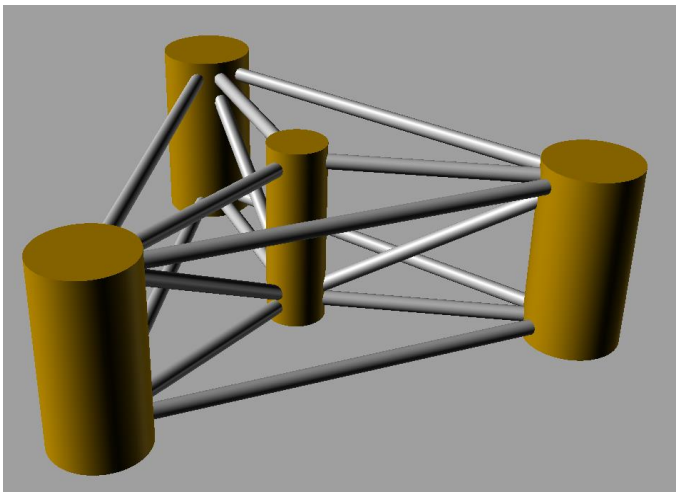

Figure 1. 3-D representation of the floating platform.

Table 1. Floating Platform Geometry.

Depth of platform base below SWL (total draft)	20.00m
Elevation of main column (tower base) above SWL	10.00m
Elevation of offset columns above SWL	10.00m
Spacing between columns	50.00m
Draft of the structure	20.00m
Diameter of main column	6.50m
Diameter of offset columns	10.00m
Diameter of pontoons and cross braces	1.60m

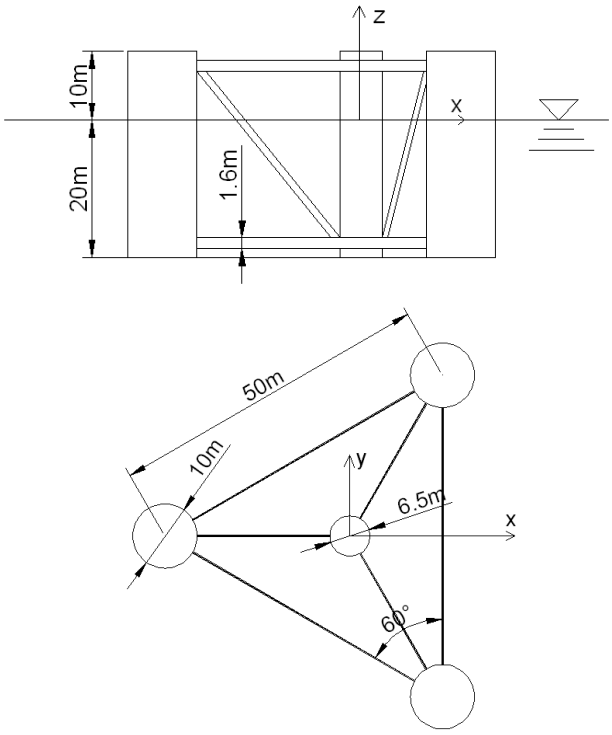

Figure 2. Front and top view of the floating platform.

The mass, including ballast, of the floating platform is 2183.6t. This mass was calculated such that the combined weight of the rotor-nacelle assembly, tower, and platform, plus the weight of the mooring system in water, balances with the buoyancy (i.e. weight of the displaced fluid) of the platform in the static equilibrium position in still water. The CM of

the floating platform, including ballast, is located at 4.05m along the platform centerline below the SWL. The roll and pitch inertias of the floating platform about its CM are 1.106E6 kg-m^2 and 1.106E6 kg-m^2 about the platform *x*-axis and *y*-axis respectively, while the yaw inertia of the floating platform about its centerline is 1.987E6 kg-m^2.

Table 2 summarizes the supporting platform's properties discussed in this section and Figure 3 illustrates the concept with an image.

Table 2. Floating Platform Geometry.

Platform mass, including ballast	2.1836t
CM location below SWL	4.05m
Platform roll inertia about CM	1.10E6 kgm^2
Platform pitch inertia about CM	1.10E6 kgm^2
Platform yaw inertia about CM	1.99E6 kgm^2

Figure 3. Representation of the floating system.

3 FORMULATION OF THE HYDRODYNAMIC PROBLEM

3.1 *Analytical solution method for the multi-body-wave interaction*

The prediction of the exciting wave forces, added masses, damping and mean drift loads, requires the knowledge of the first-order velocity potential, which, in the case of multiple cylinders, should account for hydrodynamic interaction phenomena. These phenomena have been exactly accounted for here through a semi-analytical formulation which makes use of the single body hydrodynamic characteristics in conjunction with the physical idea of multiple scattering. According to the multiple scattering formulation, various orders of propagating and evanescent wave modes radiated/scattered from all the cylinders of the array are successively superimposed to derive exact series representations for the velocity potential around each cylinder of the arrangement. The method, which is applicable to arrays consisting of an arbitrary number of vertical bodies of revolution having any geometrical arrangement and individual body geometries, has been described exhaustively in previous publications (Mavrakos et al., 1987, Mavrakos, 1991), and thus here is no further elaborated. The required first-order single body hydrodynamic characteristics have been obtained though the method of matched axisymmetric eigenfunction expansions (Kokkinowrachos et al., 1986). Here, by the way of example, the series representation for the diffraction potential, $\varphi_D^{(q)}(r_q,\theta_q,z)$, in the outer fluid region of an arbitrary body q of the multi – cylinder configuration is given:

$$\varphi_D^{(q)}(r_q,\theta_q,z) = -i\omega(H/2)\sum_{-\infty}^{\infty}\Psi_{D,m}(r_q,z)e^{im\theta_q} \quad (1)$$

With

$$\Psi_{D,m}(r_q,z) = h\sum_{n=0}^{\infty}\left[\begin{matrix} Q_{D,mn}^{(q)}\left(I_m(a_n r_q)/I_m(a_n b_q)\right)+ \\ F_{D,mn}^{(q)}\left(K_m(a_n r_q)/K_m(a_n b_q)\right)\end{matrix}\right]Z_n(z) \quad (2)$$

Where h is the water depth, b_q is the radius of the q cylinder, I_m and K_m are the *m-th* order modified Bessel functions of first and second kind, respectively. The first term in (2) represents the contribution of the incident wave field to the total wave potential around the q body. It consists of the undisturbed incident wave plus various orders of scattered waves emanating from the remaining bodies of array. These scattered wave fields can be expressed in the coordinate system of body q using a Bessel function addition theorem (Abramowitz et al., 1970).

Especially in the case of the isolated body-wave interaction, it holds:

$$Q_{D,mn}^{(q)} = \left(e^{ikl_{0q}\cos(\theta_{0q}-\beta)}/hz_0'(0)\right)e^{-im(\beta-\pi/2)}I_m(a_n b_q)\delta_{0,n} \quad (3)$$

where β denotes the angle of wave incidence, l_{0q} and θ_{0q} are the distance and the azimuthal angle of the *q-th* body co-ordinate system with respect to an inertia frame, k is the wave number and $\delta_{o,n}$ is the Kronecker's symbol.

The unknown complex coefficients $F_{D,mn}^{(q)}$ in (2) are obtained using the method of matched eigenfunction expansions (Mavrakos et al., 1987, Mavrakos, 1991). Moreover, $Z_n(z)$ are orthonormal functions in [0,-h] defined by:

$$Z_n(z) = \left\{\frac{1}{2}\left[1+\sin(2a_n h)/(2a_n h)\right]\right\}^{-1/2}\cos(a_n h) \quad (4)$$

The eigenvalues α_n are roots of the transcendental equation

$$(\omega^2/g) + a_n\tan(a_n h) = 0 \quad (5)$$

and the alternative notation α_0=-*ik* is used for the imaginary root.

3.2 *Mooring System*

To secure the platform, the floating structure is moored with a TLP mooring system of three lines spread symmetrically about the platform *Z*-axis.

The fairleads (body-fixed locations where the mooring lines attach to the platform) are located at the base of the offset columns, at a depth of 20.0m below the SWL. The anchors (fixed to the inertia frame) are located at a water depth of 200m below the SWL. Each of the 3 lines has an unstretched length of 180m, a diameter of 0.130m, an equivalent mass per unit length of 104kg/m, an equivalent apparent mass in fluid per unit length of 888.6N/m. The pretension of each tendon is 10140kN. Table 3 summarizes these properties.

The TLP, increases the vertical stiffness of the floating system, which reduces the heave period. In this way, the heave period can be shifted out of the high- energy region of the sea spectrum. From a static stability point of view, this pretension can be considered as a point mass located at the connection point of the tension leg. In addition to the resulting downward shift of the virtual center of gravity, the center of buoyancy is also moved downward in absolute sense since additional buoyancy is required to compensate the pretension.

The mooring line properties are listed in Table 3.

Table 3. Mooring System properties.

Number of Mooring lines	3	-
Depth to Anchors Below SWL (Water Depth)	200	m
Depth to Fairleads Below SWL	20	m
Mooring Line Length	180	m
Mooring Line Diameter	130	mm
Equivalent Mooring Line Mass Density	104	kg/m
Equivalent Mooring Line Mass in Water	888.6	N/m
Mooring Line stiffness k_{xx} of each tendon	56.33	kN/m
Mooring Line stiffness k_{ZZ} of each tendon	14700	kN/m
Pretension of each tendon	10140	kN

To summarize, the tether tension for this system must fulfill three requirements: (1) the tethers must provide sufficient restoring in surge to adequately limit the steady-state offset in surge; (2) the tension of the windward tether must never exceed the maximum allowable tension, and the leeward tether must never go slack or fall below the minimum allowable tension at any point during operation; and (3) the total pretension force exerted by the tethers must match the weight of the water required to ballast the system for stability during installation.

3.3 *Reduced modeling of the Wind Turbine*

The gravitational, inertial and aerodynamic loads that the WT contributes on the floater dynamics are defined in the simplest possible way; with respect to gravitational and inertial loading, the wind turbine is modeled as a collection of concentrated masses, namely the masses of the blades, the hub, the nacelle and the tower. The aerodynamic loading is first calculated as a distribution along the blades and then transferred at the positions of the blade masses.

Let $\mathbf{q}$ denote the vector of the 6 floater motions, following the formalism of Lagrangian equations, the relevant terms (see eq. 9) are obtained:

$$\frac{d}{dt}\left(\frac{\partial L}{\partial \dot{q}_i}\right)-\left(\frac{\partial L}{\partial q_i}\right)=Q_i=\sum_j \frac{\partial\left(\mathbf{f}_j\cdot\mathbf{r}_j\right)}{\partial q_i} \quad L=L\left(\mathbf{q},\dot{\mathbf{q}}\right) \tag{6}$$

where L denotes the Lagrangian and $\mathbf{Q}$ generalized external loads (aerodynamic, gravity).

Aerodynamic modeling in the BEM context is defined on the basis of the effective angle of attack α and the effective relative velocity U_{eff} (Figure 4), which determine the loads (sectional lift and drag C_L, C_D or normal and tangent forces C_n, C_t) using look up tables. Their definition includes the wind inflow U_W, the rotational speed Ω, the blade pitch β_p that is added to the local twist angle θ_t and the induction factors a, a′. In the present case, along the blade, the velocity components $\delta U_a, \delta U_c$ induced by the floater motions must be also added. They will be functions of $\mathbf{q}, \dot{\mathbf{q}}$.

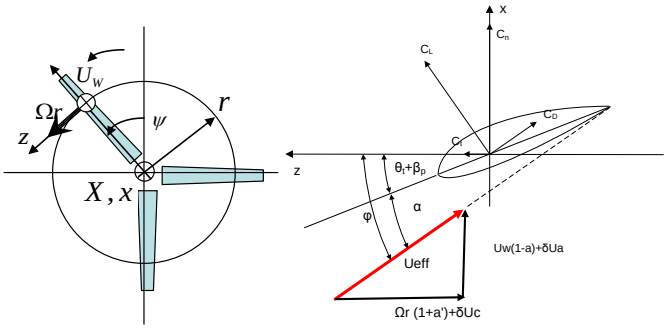

Figure 4: Definition of the aerodynamic set-up

The framework for calculating the aerodynamic loads is by construction non-linear, so in order to define a reduced order model, linearization is needed. The usual approach is to consider small perturbations with respect to a reference state. Choosing as reference state the static positioning of the system at a specific wind speed without wave loading, linearization consists of assuming:

$$\mathbf{Q}=\mathbf{Q}_0+\partial_q\mathbf{Q}\delta q+\partial_{\dot{q}}\mathbf{Q}\delta\dot{q} \tag{7}$$

and determining the coefficients of δq, $\delta\dot{q}$ using the information at the reference state. To this end, it is assumed that the aerodynamic coefficients (next only the lift coefficient is shown), are defined as follows:

$$C_L=C_{L0}+\partial_\alpha C_L\delta\alpha, \quad \delta\alpha=\partial_q\alpha.\delta q+\partial_{\dot{q}}\alpha\cdot\delta\dot{q} \tag{8}$$

In the above, the derivatives of the aerodynamic coefficients are readily obtained from the look up tables, while the derivatives of the angle of attack with respect to the q's are obtained through $\delta U_a, \delta U_c$

4 COUPLED ANALYSIS

4.1 *Response Amplitude Operators*

The frequency-domain software HYDRAERO-FLOAT was developed by the first author (Mazarakos et al., 2014) for coupled analysis of floating structures. It uses HAMVAB (Mavrakos, 1996) and ROM (Papadakis et al., 2014), as preprocessors to compute wave interaction effects and computes the frequency-domain response of one or more floaters subjected to waves, wind, and connected with moorings, tendons, or any other mechanical connections.

The RAO's are calculated for the combined wind turbine and floating platform system. The equations of motion that govern the linear dynamic motions of the system are summarized in matrix form:

$$\left[M_{ij}^{structure}+A_{ij}^{structure}(\omega)+M^{WT}\right]\ddot{x}+\left[B_{ij}^{structure}(\omega)+B_{ij}^{WT}\right]\dot{x}+\left[C_{ij}^{structure}+C_{moorings}+C_{ij}^{WT}\right]x=F(\omega)e^{i\omega t} \quad (9)$$

The superscripts *structure* and *WT* corresponds to physical quantities associated with the floating structure and the wind turbine, respectively. In particular, M_{ij} is the mass of the floating structure, A_{ij}, B_{ij}, and C_{ij} represent its 6 by 6 added mass, damping, and stiffness matrices, respectively, and $F(\omega)e^{i\omega t}$, the six by one vector that contains the hydrodynamic exciting forces. These matrices are calculated by the HAMVAB module (superscript *structure*) for the floating platform and in Eq. 9 are superposed to the matrices calculated by the ROM (superscript *WT*) for the wind turbine. The restoring matrixes *C*, include contributions from hydrostatics, moorings and *WT*, as developed in the previous section.

The symbol x represents the system's dimensional response in each mode of motion at each frequency. Because of the nonlinear nature of the aerodynamics and dynamics, it is not possible to define M^{WT}, B^{WT} and C^{WT} for all wind speeds. The rotor speed, the mean pitch reference angle and the induction factors a and a' refer to the reference state which is defined for every wind speed. So the RAO's of the combined system depends on the wind speed.

4.2 *Advanced full hydro-servo-aero-elastic modeling of the system*

The behavior of floating wind turbines is considered in the context of the dynamics of the whole construction subjected to external forcing and appropriate constraints. External forcing includes the aerodynamic loading on the rotor blades due to the wind inflow, the gravitational loads and the hydrodynamic loading on the floater and the mooring lines. Structural modeling is based on the multi-body approach. The wind turbine is divided in its components, which are either rigid (the floater) or flexible (blades, tower, drive train). Flexible components are modeled as beams subjected to combined bending in two directions, tension and torsion. Currently, 2 options are available in hydroGAST, a 2nd order Euler Bernoulli beam model and a linear Timoshenko beam model. The latter is used in this work. The floater is modeled as a rigid body connected to the wind turbine at the bottom of the tower. The position of the floater is defined by its 6 rigid body motions (3 translations and 3 rotations), which are constrained by the mooring lines. A dynamic mooring line model is used that considers the mooring lines as one-dimensional flexible components transmitting axial loads. Co-rotating non-linear truss elements are used in the FEM context.

As mentioned in the introduction, hydroGAST has been defined in a fully coupled and non-linear context. In this sense, time domain simulations perform iterations per time step until the errors of all sub models converge. In the context of floating wind turbines the following couplings are considered:

a) The motions of the floater are added as rigid body motions through the multi-body formulation in addition to the deformation velocities which together affect the aerodynamic performance of the blades through the effective angle of attack. In doing so the system receives as feedback the eventual aerodynamic damping.

b) The aerodynamic loads are transmitted to the structural modeling together with the wave loading and determine the motions of the floater which is also subjected to the reaction loads of the moorings.

c) The controller receives as input the performance characteristics and feeds back the blade pitch and/or the rotational speed.

5 NUMERICAL RESULTS

5.1 *Eigen values*

In Table 4 the eigenvalues of the coupled system are given for the rigid and flexible ("flex") cases. The main difference in the "flex" data is the shifting of the roll/pitch eigenvalues and the presence of the tower fore-aft and side-to-side frequencies at 0.244 Hz.

Table 4. Eigen frequencies of the coupled system.

dof	rigid case [Hz]	flex case [Hz]
Surge	0.026	0.026
Sway	0.026	0.026
Heave	0.573	0.572
Roll	0.301	0.864
Pitch	0.301	0.857
Yaw	0.028	0.028
1st tower	-	0.244
1st tower fore	-	0.245

5.2 *RAO's of the coupled system*

The RAO's can be estimated from time series data from the following equation:

$$RAO(\omega) = \frac{|P_{xy}(\omega)|}{P_{xx}(\omega)} \quad (10)$$

where P_{xx} is the auto power spectral density and P_{xy} is the cross spectral density. P_{xx}, P_{xy} are calculated using Welch's method (Welch, 1967) with a sufficient number of data split and 50% overlap between the split data parts. *x* refers to the input (wave elevation) and *y* to the output (each motion). The simulations lasted 3600sec - the first 600sec are excluded – assuming a uniform wind speed and white noise waves of 1m significant wave height.

First, in Figures 5-7 the zero wind speed case with zero degree wave heading is presented. Two sets of time domain calculations are included: one corresponding to a rigid WT and one with a flexible one. Only the 3 excited motions, i.e. surge, heave and pitch, are presented. Frequency and time domain results are consistent, although the frequency domain method predicts larger amplitudes near resonance. Lack of viscous damping and dynamic nonlinearities could explain this difference, but further study is needed. RAO's amplitude is very sensitive in the damping modeling. The flexibility of the WT is important only in the pitch RAO (tower peak at 0.25Hz), while the pitch frequency is not present because of the shift from 0.3Hz to 0.86Hz (see Table 4).

Next, RAO's were computed for wind speeds of 0 m/s, 8m/s, 11.4m/s and 18m/s and for wave heading of 0 degrees and 30 degrees. Results are only presented for the 30degrees case (Figures 8-13) because in this case all motions are excited. Again the predictions are consistent. The peak amplitudes obtained with the frequency method are higher while the flexibility of the WT only affects the roll and the pitch motions, due to the strong coupling with the tower modes. The tower frequency is also depicted in the yaw motion, but with low energy. The aerodynamic damping and the gyroscopic effects are captured by both methods, as also reported for the spar-buoy case (Ramachandran et al., 2013). For example in surge, roll and pitch motions, the presence of the wind, reduces the peaks, while the yaw peak increases due to the gyroscopic effect. These effects are considered in frequency domain through the WT matrices in linearized context. Minor differences between the two methods with respect to the wind speed influence could be linked to the nonlinearities which are present in the time domain simulations: dynamic inflow and aerodynamic damping in the BEM calculations, as well as nonlinear dynamics.

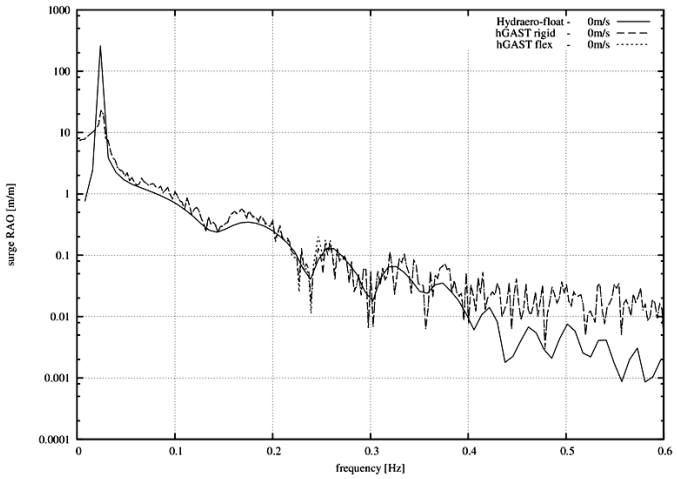

Figure 5. Surge motion of the TLP combined floating platform and wind turbine system. Wave heading 0 degrees and no wind.

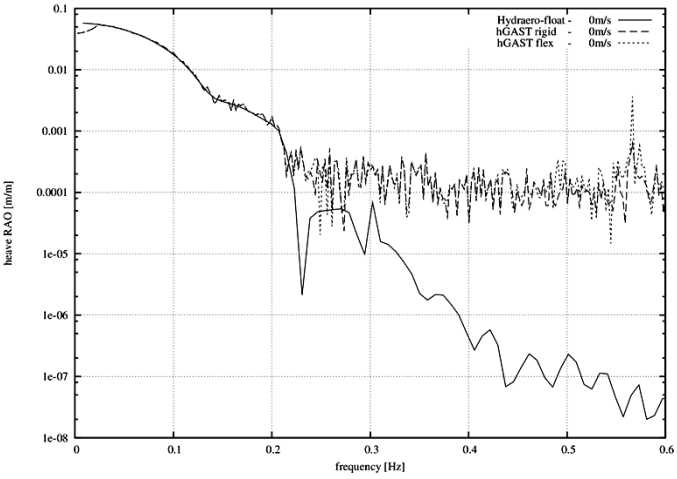

Figure 6. Heave motion of the TLP combined floating platform and wind turbine system. Wave heading 0 degrees and no wind.

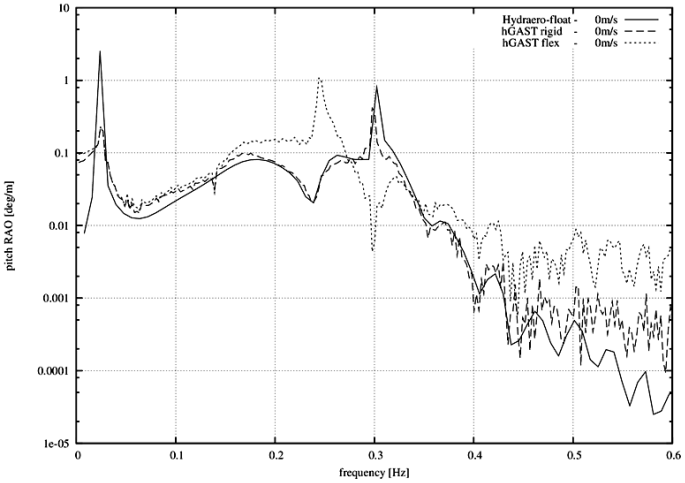

Figure 7. Pitch motion of the TLP combined floating platform and wind turbine system. Wave heading 0 degrees and no wind.

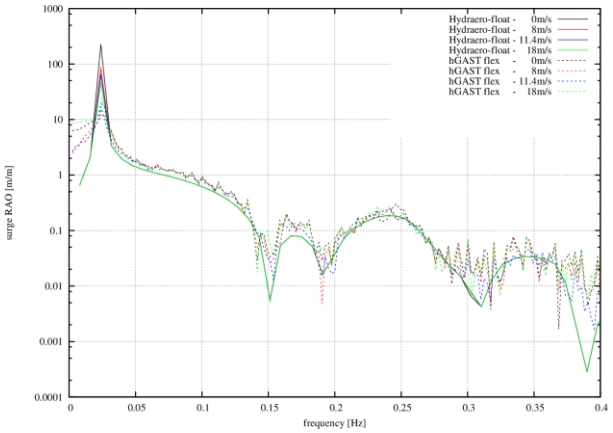

Figure 8. Surge motion for wave heading 30 degrees.

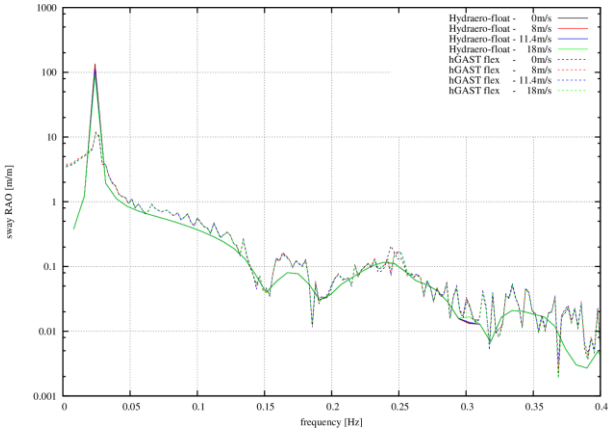

Figure 9. Sway motion for wave heading 30 degrees.

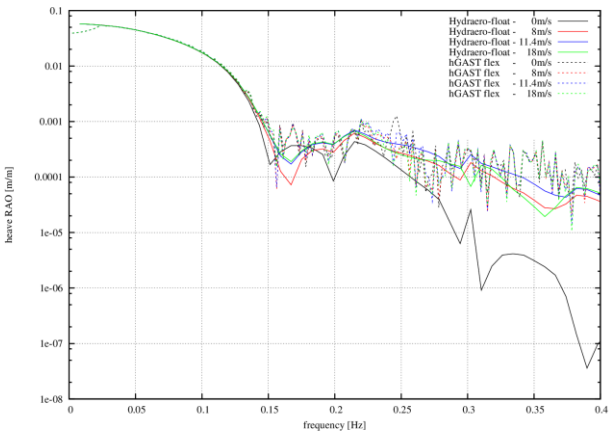

Figure 10. Heave motion for wave heading 30 degrees.

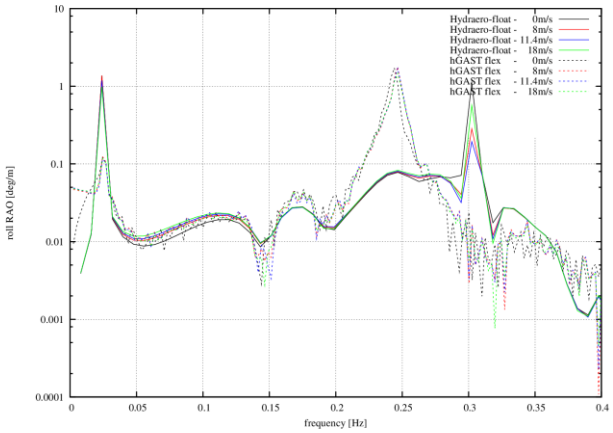

Figure 11. Roll motion for wave heading 30 degrees.

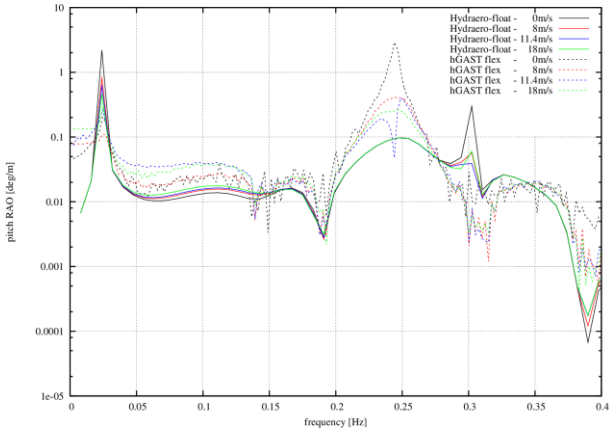

Figure 12. Pitch motion for wave heading 30 degrees.

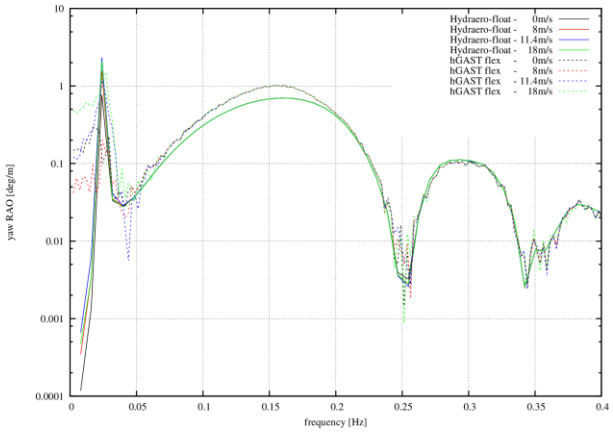

Figure 13. Yaw motion for wave heading 30 degrees.

6 CONCLUSIONS

A TLP floater for the NREL 5MW RWT has been presented with 3 cylinders, which will at a later stage include 3 OWC devices. For the present work, the WT characteristics were not modified, although the tower should become stiffer.

For this design, RAO's of the complete system have been calculated using on one hand a frequency domain method based on a ROM model for the WT, and on the other with an advanced fully coupled method producing time domain simulations that can also take into account the flexibility of the system components.

By comparing the results from the two methods, the following conclusions were drawn:

1. Both methods consistently predict the system RAO's, which gives confidence to the specific frequency domain approach as a preliminary design tool. This is so even for the pitch motion which in time domain calculations does not exceed 0.1deg.
2. The frequency domain method does not include structural flexibilities which affect the roll/pitch RAO's. The natural frequency in roll/pitch for the rigid WT is 0.3Hz, while for the flexible WT is 0.85Hz and the tower bending frequencies about 0.24Hz. On the other hand roll and pitch is very small for a TLP and not within the wave frequency range. In any case adding a small number of structural eigenmodes in the dynamic system is not expected to increase the computational cost and could be considered in view of improving the ROM modeling.
3. Because of the strong coupling between the floater roll/pitch motions and the tower fore-aft and side-to-side bending, the stiffness of the tower should be increased in the next design revision – the current natural frequency is about 0.24Hz, and should become ~0.45Hz in order to be out of the wave frequency range.
4. The RAO's amplitudes near resonance as predicted by the time domain method are smaller due to viscous damping and other nonlinearities. The amplitudes are very sensitive to the damping and this should be further investigated.
5. Aerodynamic damping clearly reduces the amplitude of the motions around the resonance, while the gyroscope effect increases the yaw amplitude.

7 FUNDING AND ACKNOWLEDGEMENTS

This research has been co-financed by the European Union (European Social Fund– ESF) and Greek national funds through the Operational Program "Education and Lifelong Learning" of the National Strategic Reference Framework (NSRF) 2007– 2013: Research Funding Program: ARISTEIA, Program POSEIDON (2041).

8 REFERENCES

Abramowitz, M., Stegun, I.A. 1970. *Handbook of Mathematical Functions*. 9th Ed. Dover Publications.

Goupee, A.J., Koo, B.J., Lambrakos, K.F. and Kimball, R.W. 2012. Model Tests for Three Floating Wind Turbine Concepts," *Offshore Technology Conference*.

Jonkman, J., Butterfield, S., Musial, W. and Scott G. 2009 Definition of a 5-MW Reference Wind Turbine for Offshore System Development, Technical Report, NREL/TP-500-38060, USA.

Jonkman, J. 2010. Definition of the Floating System for Phase IV of OC3, Technical Report NREL/TP-500-47535, USA,.

Jonkman, J., Musial W., 2010. Final Report, Subtask 2, The Offshore Code Comparison Collaboration (OC3), IEA Wind Task 23.

Kokkinowrachos, K., Mavrakos, S.A., Asorakos, S. 1986. Behavior of vertical bodies of revolution in waves. *Ocean Engineering*, 13, pp. 505-538.

Manolas, D., Riziotis, V., Voutsinas, S., 2012. Assessment of 3D aerodynamic effects on the behaviour of floating wind turbines, *The science of making torque from Wind, TORQUE 2012*, Oldenbourg, Germany.

Manolas, D., Riziotis, V., Voutsinas, S., 2014. Assessing the importance of geometric non-linear effects in the prediction of wind turbine blade loads, (*submitted for publication to ASME JSE*)

Mavrakos, S.A., Koumoutsakos, P. 1987. Hydrodynamic interaction among vertical axisymmetric bodies restrained in waves. *Applied Ocean Research*, 9, pp. 128-140.

Mavrakos, S.A. 1991. Hydrodynamic coefficients for groups of interacting vertical axisymmetric bodies. *Ocean Engineering*, 18, pp. 485-515.

Mavrakos, S.A. 1996. User's Manual for the softwere HAMVAB, School of Naval Architecture and Marine Engineering, Laboratory for Floating Structures and Mooring Systems.

Mazarakos, T.P., Mavrakos, S.A., Konispoliatis, D.N., Voutsinas, S.G., Manolas, D. 2014. Multi- purpose floating structures for offshore wind and wave energy sources exploitation. *COCONET Workshop for Offshore Wind Farms in the Mediterranean and Black Seas, Anavyssos- Greece, 9- 10 June 2014.*

Papadakis, G., Riziotis, V., Voutsinas, S., Mavrakos, S.A. 2014. W/T's reduced order aeroelastic models (in Greek). Technical Report No. D3.2, Program POSEIDON (2014), Greek General Secretariat for Research and Technology.

Ramachandran G., Robertson, A., Jonkman, J. and Masciola, M. D., 2013. Investigation of Response Amplitude Operators for Floating Offshore Wind Turbines Preprint, *ISOPE 2013 Anchorage, Alaska*.

Riziotis. V.A., Voutsinas, S.G. 1997. GAST: A general aerodynamic and structural prediction tool for wind turbines. Procerdings of the EWEC' 97, Dublín, Ireland, 1997.

Riziotis, V., S.G. Voutsinas, E.S. Politis, P.K. Chaviaropoulos 2004. Aeroelastic Stability of Wind Turbines: the problem, the methods, the issues", *Wind Energy*, 7, pp 373-392

Robertson Amy et al., 2014. Offshore code comparison collaboration, continuation within IEA wind task 30: phase II results regarding a floating semisubmersible wind system, *OMAE 2014, San Francisco, USA.*

Sclavounos, P.D., Wayman, E.N., 2006. Coupled Dynamic Modelling of Floating Wind turbine Systems. *Offshore Technology Conference, Texas, 2006.*

Stewart, G., Lackner, M., Robertson, A. and Jonkman, J., 2012. Calibration and Validation of a FAST Floating Wind Turbine Model of the DeepCwind Scaled Tension-Leg Platform, *22nd International Offshore and Polar Engineering Conference Rhodes, Greece, June 17-22, 2012.*

Welch, P.D., 1967. The Use of Fast Fourier Transform for the Estimation of Power Spectra: A Method Based on Time Averaging Over Short, Modified Periodograms, *IEEE Transactions on Audio Electroacoustics,* AU-15, 70–73.